



# IMPACT DAMPING WITH GRANULAR MATERIALS IN A HORIZONTALLY VIBRATING SYSTEM

M. SAEKI

*Department of Mechanical and Control Engineering, Niigata Institute of Technology, Fujihashi,  
Kashiwazaki, Niigata 945-1195, Japan. E-mail: saeki@mce.niit.ac.jp*

*(Received 29 May 2001, and in final form 24 August 2001)*

The damping efficiency of an impact damper with granular materials in a horizontally vibrating system is investigated by means of the discrete element method. This method makes it possible to consider effects of granularity such as the particle size, number of particles and friction between two particles. The validity of this numerical method is examined by a comparison of the experimental results. It is shown that the mass ratio, particle size and cavity dimensions influence the damping performance. It is also shown that the cavity dimensions and the particle radius affect the behavior of the granular materials.

© 2002 Elsevier Science Ltd.

## 1. INTRODUCTION

Impact damping is a passive vibration control technique that consists of an impactor operating in the cavity of a primary system. Each collision of the impactor with the wall of the cavity results in an exchange of momentum and some energy dissipation, producing attenuations of the response of the primary system. Due to the simplicity of their construction, impact dampers have been widely used for structural damping applications in skyscrapers, machine tools and other lightly damped structures. Impact dampers have also been considered for use in harsh environments such as turbo machinery blade, since their effectiveness is independent of the environment. A solid particle has conventionally been used as the impactor [1]. However, the significant impact force may result in high noise levels and surface degradation. Sato *et al.* reported that these problems may be reduced by means of granular materials instead of the single particle [2].

Impact dampers with granular materials have been the subject of several analytical and experimental studies. Araki *et al.* [3] investigated the characteristics of impact dampers with granular materials in a single-degree-of-freedom system that was subjected to an external sinusoidal force. Papalou and Masri [4] studied impact dampers in a horizontally vibrating system under random excitation. They investigated the effects of mass ratio, particle size, container dimensions and excitation levels on the performance of the system. Yokomichi *et al.* [5] investigated the influence of granular materials in a multibody vibrating system. Friend and Kinra [6] developed an elementary analytical model to predict impact damping with granular materials. They showed that good agreement was obtained between the analytical and experimental results.

Although all of these papers present the damping effects when granular materials are used, these investigations have not yet been completed. Most previous theoretical analyses have focused on the concept of an equivalent single-particle impact damper.

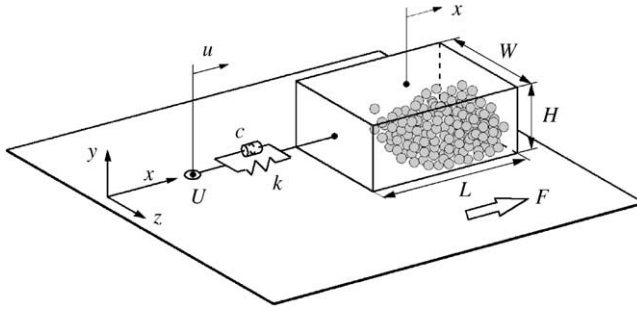


Figure 1. Model of an impact damper with granular materials.

This paper investigates the damping efficiency of an impact damper with granular materials in a horizontally vibrating system under sinusoidal excitation. The objective of this work is to investigate the influence of mass ratio, particle size and cavity dimensions on the damping performance by means of a novel analytical method based on the discrete element method (DEM) [7]. This method makes it possible to consider the effects of granularity such as the particle size, number of particles and friction between two particles. The validity of the theory was confirmed by a comparison of experimental and analytical results. In addition, the flow pattern of granular materials is presented.

## 2. IMPACT DAMPER WITH GRANULAR MATERIALS

Figure 1 shows the model of an impact damper with granular materials. In this figure, the  $x$ - $z$  plane is parallel to the horizontal plane. The primary system consists of a mass  $M$ , a spring  $k$  and a damper with damping constant  $c$ , which is assumed to move only along the direction of the  $x$ -axis. The primary system is excited by the motion of the support point  $U$ . When granular materials are placed in the cavity of the primary system as shown in Figure 1, the collision of the particles with the wall of the cavity results in a reduction of the amplitude of the primary system through momentum transfer. By letting  $u$  and  $x$  be the harmonic displacement of the support point  $U$  and the displacement of the primary system, respectively, the equation of motion for the primary system is given by

$$M\ddot{x} + c\dot{x} + kx = c\dot{u} + ku + F, \quad u = a \sin \omega t, \quad (1)$$

where  $F$  is the component of the contact force acting on the primary system in the direction of the  $x$ -axis, and  $a$  and  $\omega$  are the amplitude and the angular frequency of the harmonic vibrating support point respectively. The cavity of the primary system is box-like with length  $L$ , height  $H$ , and width  $W$ ;  $L$ ,  $H$  and  $W$  are parallel to the  $x$ ,  $y$  and  $z$  directions, respectively, as shown in Figure 1.

## 3. EXPERIMENTAL SET-UP AND SYSTEM RESPONSE

A schematic of the experimental apparatus is shown in Figure 2. The experimental model consisted of the primary structure and the granular materials. The structure is made of acrylic resin and is supported by two leaf springs, acting as a single-degree-of-freedom system. The dimensions of the cavity are  $L = 58$  mm,  $H = 38$  mm and  $W = 38$  mm. The

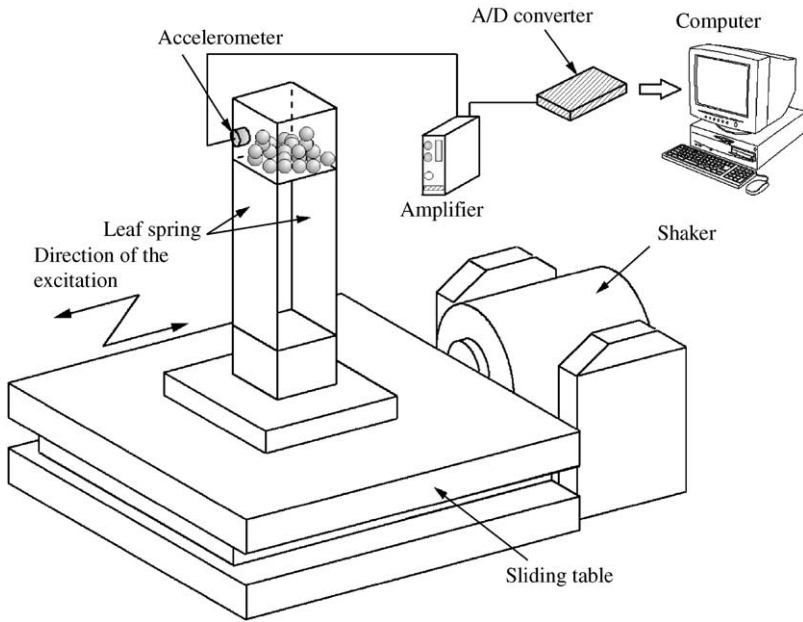


Figure 2. Schematic of the experimental apparatus.

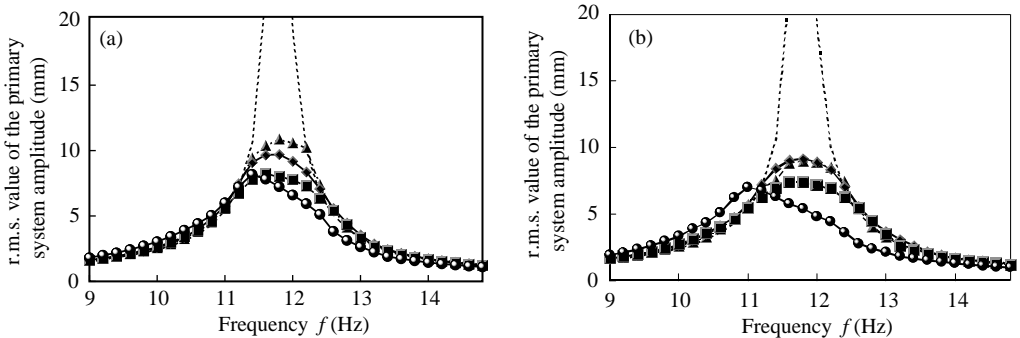


Figure 3. Influence of the particle material on the frequency response of the primary system ( $a = 1.0$  mm). (a)  $\lambda = 0.092$ ; (b)  $\lambda = 0.138$ ; -----, no damper; ---▲---, lead; ---◆---, SUS304; ---■---, Steel; ---○---, Acrylic resin.

system was excited at the support of the structure by means of a horizontally vibrating shaker. The equivalent properties of this system were found to be  $M = 0.293$  kg,  $c = 0.116$  N s/m and  $k = 1602.7$  N/m. An accelerometer was used to measure the motion of the primary system. To investigate the effect of the particle material on the damping efficiency, the following granular materials were used as impactors: lead, SUS304, steel and acrylic resin. In this study, an assembly of spherical particles of uniform size and density is used.

Figures 3(a) and 3(b) show plots of the root mean square (r.m.s.) value of the primary system amplitude versus the frequency  $f$  of the vibrating support ( $f = \omega/2\pi$ ). In these figures,  $\lambda$  is the mass ratio, which is the total mass of granular materials per mass of the primary system. In cases (a) and (b), the mass ratios  $\lambda$  are 0.092 and 0.138, respectively. It is clear that damping is efficient in the presence of granular materials. The response of the primary

system depends on the particle material. More importantly, the maximum amplitude of acrylic resin particles occurs at the lowest frequency, and the reason appears to be that the total volume of acrylic resin particles is the largest due to the difference in density.

#### 4. NUMERICAL METHOD

The dynamics of the impact damper is complex. In order to capture the behavior of the entire system in detail, the equation of motion for each particle must be solved, considering the interactive effects due to friction and to collision between two particles or a particle and the wall of the cavity. The equation of motion for a particle  $i$  is given by

$$m_i \ddot{\mathbf{p}}_i = \mathbf{F}_i - m_i \mathbf{g}, \quad I_i \dot{\boldsymbol{\varphi}}_i = \mathbf{T}_i, \quad (2)$$

where  $m$  is the particle mass,  $I$  is the moment of inertia of the particle, and  $\mathbf{g}$  is the acceleration vector due to gravity.  $\mathbf{p}$  is the position vector of the center of gravity of the particle,  $\boldsymbol{\varphi}$  is the angular velocity vector, and  $\mathbf{F}$  is the summation of the contact forces acting on the particle.  $\mathbf{T}$  is the summation of the torque caused by the contact forces. The dots denote a time derivative.

Figure 4 shows the contact state between the two particles  $i$  and  $j$ . In this figure,  $P_i$  and  $P_j$  denote the centers of  $i$  and  $j$ , and  $C$  is the contact point. Next, consider the normal component  $F_N$  and tangential component  $F_T$  of the contact force. The normal component  $F_N$  of the contact force is modelled by the sum of the spring force based on Hertzian contact theory and the damping force  $D_N$  [7] and is expressed by

$$F_N = k_N \delta_N^{3/2} + D_N, \quad (3)$$

where  $\delta$  and  $\dot{\delta}$  are the displacement and velocity of particle  $i$  relative to particle  $j$  respectively.  $k_N$  is the spring constant, and  $c_N$  is the damping coefficient. In cases of interparticle contact and particle contact with the wall, normal displacement  $\delta_N$  is given by

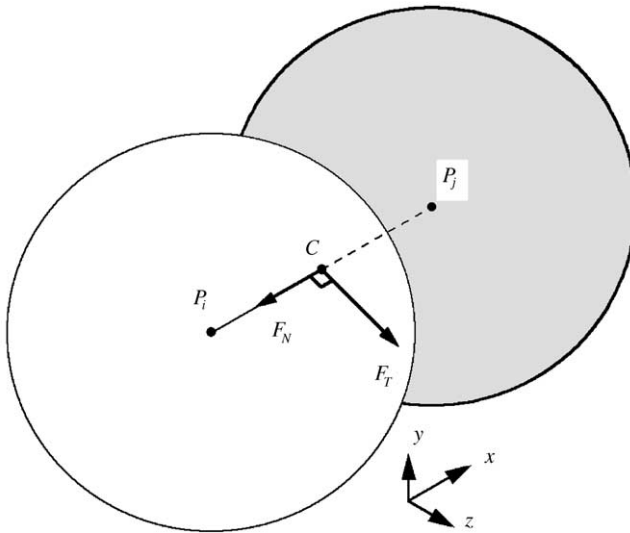


Figure 4. Contact state between two particles,  $i$  and  $j$ .

equations (4) and (5) respectively.

$$\delta_N = r_i + r_j - |\mathbf{p}_j - \mathbf{p}_i|, \quad \delta_N = r_i - t, \quad (4, 5)$$

where  $r$  and  $t$  are the particle radius and the distance from the center of the particle to the wall respectively. Subscripts  $i$  and  $j$  denote the two particles  $i$  and  $j$ .

By means of the Hertzian theory of elastic contact for spheres, the spring constant  $k_N$  in equation (3) is expressed as

$$k_N = \frac{4}{3} \sqrt{\frac{r_i r_j}{r_i + r_j}} \frac{E_i E_j}{(1 - v_i^2) E_j + (1 - v_j^2) E_i}, \quad (6)$$

where  $E$  and  $v$  are the modulus of elasticity and the Poisson ratio respectively. In the case of contact between a sphere and the wall,  $k_N$  is expressed as

$$k_N = \frac{4\sqrt{r_i}}{3} \frac{E_i E_0}{(1 - v_i^2) E_0 + (1 - v_0^2) E_i}, \quad (7)$$

where subscript 0 denotes the wall.

As for the damping force  $D_N$  in equation (3), Tsuji *et al.* [8] proposed the following equation:

$$D_N = \alpha \sqrt{mk} \delta_N^{1/4} \dot{\delta}_N. \quad (8)$$

When the damping force  $D_N$  is defined by equation (8), the damping constant  $\alpha$  is a function of the coefficient  $e$  of restitution. Therefore, the value of  $\alpha$  is determined by the coefficient  $e$  of restitution.

The tangential component  $F_T$  of the contact force is given in equation (9), considering Coulomb's law of friction.

$$F_T = -\mu f_N \dot{\delta}_T / |\dot{\delta}_T|, \quad (9)$$

where  $\mu$  is the coefficient of friction between two particles or between a particle and the wall of the cavity. In this study, the adhesive force between two particles is neglected. Each particle may be in contact with many particles and the wall simultaneously. Therefore, the summation  $\mathbf{F}$  of the contact force acting on the particle and the summation  $\mathbf{T}$  of the torque caused by the contact force are given by

$$\mathbf{F}_i = \sum (\mathbf{f}_N + \mathbf{f}_T), \quad (10)$$

$$\mathbf{T}_i = \sum (r_i \mathbf{n}_{ij} + \mathbf{f}_T), \quad (11)$$

where  $\mathbf{n}_{ij}$  is the unit vector from the center of particle  $i$  to the center of particle  $j$ .

Here, the procedure for calculating the behavior of the impact damper used in this study is described. First, consider the motion of a particle and determine the contact force acting on the particle from equations (3–9). By using this force, the contact force  $\mathbf{F}$  and the torque  $\mathbf{T}$  caused by the contact force are obtained using equations (10) and (11). Then, the particle motion is analyzed using equation (2). The same procedure is repeated for all the particles. In addition, the component of the contact force  $F$  acting on the primary system in the  $x$ -axis (Figure 1) is given by the summation of the contact forces between the particles and the wall

of the cavity. By using the component of the contact force  $F$ , the equations of motion for the primary system (equation (1)) are analyzed.

### 5. ANALYTICAL RESULTS

In this section, the effect of the system parameters on the damping efficiency is investigated in terms of the analytical results. The computational conditions used for the simulation were identical to those applied in the experiment. Table 1 lists the computational conditions for granular materials. The particle properties correspond to those of acrylic resin.

Figures 5(a) and 5(b) show the comparison of experimental results with calculated ones in the same plane as Figure 3. In cases (a) and (b), the amplitudes  $a$  are 0.5 and 1.0 mm respectively. As shown in these figures, it is clear that the calculated results show an experimental trend with reasonable accuracy. Therefore, the approach of this study is very effective for capturing the dynamics of impact dampers with granular materials.

Figures 6(a)–(c) show examples of the behavior of granular materials in the cavity. It is clearly observed that, as time passes, granular materials move between two ends of the cavity. In the case of Figure 6(b), the cavity length  $L$  is smaller than that in the case of Figure 6(a). From a comparison of Figures 6(a) and 6(b), the number of particles which make contact with the floor of the cavity increases as the cavity length  $L$  increases. In the case of Figures 6(a) and 6(c), the particle radii are 3.0 and 6.5 mm respectively. From a comparison

TABLE 1

*Values of parameters in granular materials*

Total number	200–300
Diameter (mm)	6
Density ( $\text{kg/m}^3$ )	1190
Coefficient of friction $\mu$	0.52
Damping constant $\alpha$	0.077
Spring constant ( $\text{N/m}^{3/2}$ )	Particle–particle Particle–wall
	$1.0 \times 10^7$ $1.3 \times 10^7$

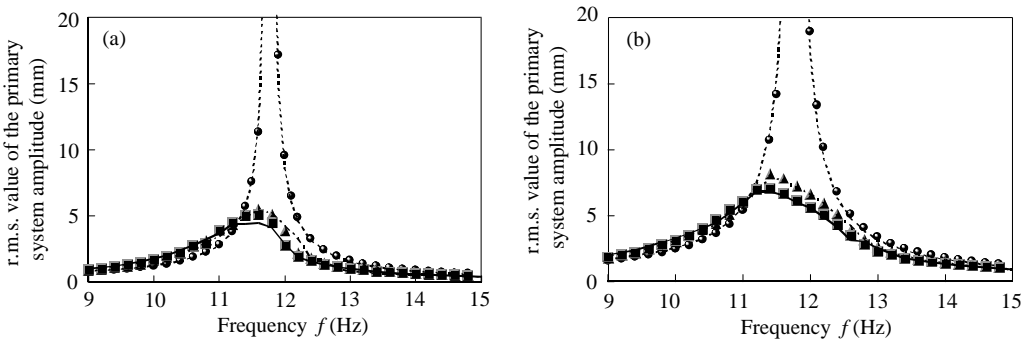


Figure 5. Comparison between experimental and calculated results ( $L = 58$  mm,  $W = H = 38$  mm,  $r = 3.0$  mm): (a)  $a = 0.5$  mm; (b)  $a = 1.0$  mm. Experimental:  $\bullet$ , No damper;  $\blacktriangle$ ,  $\lambda = 0.092$ ;  $\blacksquare$ ,  $\lambda = 0.115$ . Calculated: -----, No damper; - · - · - ·,  $\lambda = 0.092$ ; —,  $\lambda = 0.115$ .

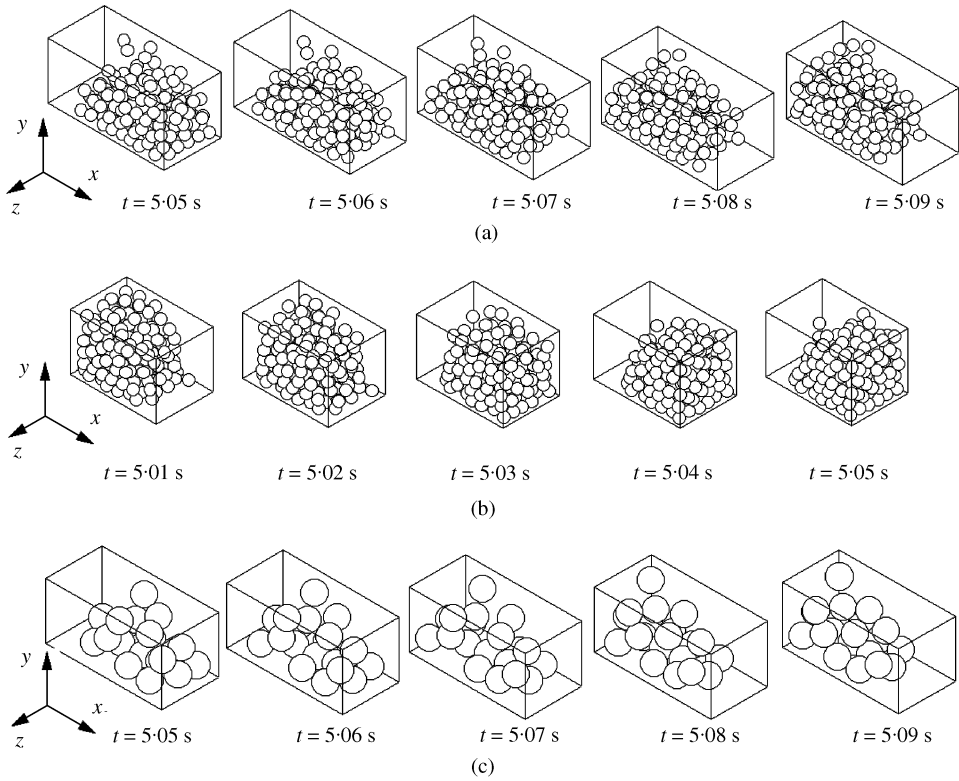


Figure 6. Behavior of granular materials ( $a = 1.0$  mm,  $f = 11.2$  Hz): (a)  $L = 78$  mm,  $W = H = 38$  mm,  $N = 200$ ,  $r = 3.0$  mm; (b)  $L = 58$  mm,  $W = H = 38$  mm,  $N = 200$ ,  $r = 3.0$  mm; (c)  $L = 78$  mm,  $W = H = 38$  mm,  $N = 20$ ,  $r = 6.5$  mm.

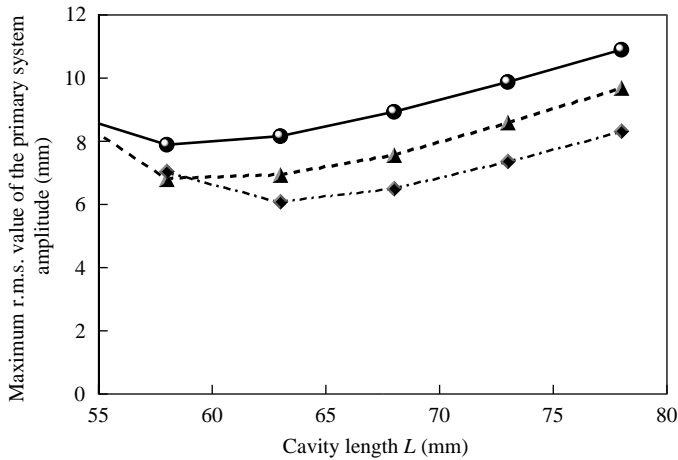


Figure 7. Influence of the mass ratio on the damping efficiency ( $W = H = 38$  mm,  $r = 3.0$  mm,  $a = 1.0$  mm):  $\bullet$ — $\bullet$ ,  $\lambda = 0.092$ ;  $\blacktriangle$ - - - $\blacktriangle$ ,  $\lambda = 0.115$ ;  $\blacklozenge$ - · - · $\blacklozenge$ ,  $\lambda = 0.138$ .

of Figures 6(a) and 6(c), it appears that it is easy for granular materials to be in contact with both the wall and each other simultaneously, as the particle radius decreases.

Figure 7 shows the relationship between the maximum r.m.s. value of the primary system amplitude and the cavity length  $L$ . Figure 7 also shows the effect of the mass ratio on the

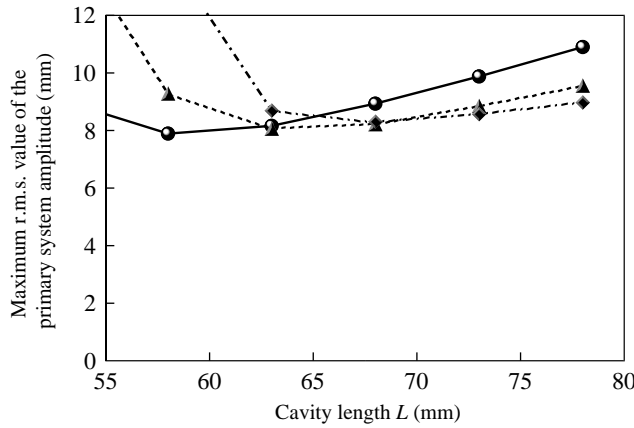


Figure 8. Influence of the particle radius on the damping efficiency ( $W = H = 38$  mm,  $\lambda = 0.092$ ,  $a = 1.0$  mm):  $\bullet$ — $\bullet$ ,  $r = 3.0$  mm;  $\blacktriangle$ — $\blacktriangle$ ,  $r = 5.0$  mm;  $\blacklozenge$ — $\blacklozenge$ ,  $r = 6.5$  mm.

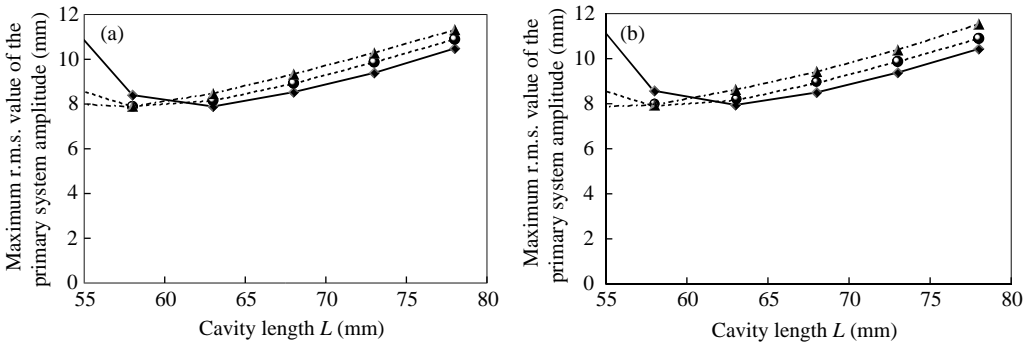


Figure 9. Influence of the cavity dimensions on the damping efficiency ( $\lambda = 0.092$ ,  $a = 1.0$  mm). (a) Effect of the cavity height ( $W = 38$  mm):  $\bullet$ — $\bullet$ ,  $H = 33$  mm;  $\blacklozenge$ — $\blacklozenge$ ,  $H = 38$  mm;  $\blacktriangle$ — $\blacktriangle$ ,  $H = 48$  mm. (b) Effect of the cavity width ( $H = 38$  mm):  $\bullet$ — $\bullet$ ,  $W = 33$  mm;  $\blacklozenge$ — $\blacklozenge$ ,  $W = 38$  mm;  $\blacktriangle$ — $\blacktriangle$ ,  $W = 48$  mm.

response of the primary system. The response of the primary system decreases with the increase of the mass ratio. It is also evident that a higher mass ratio results in the increase of the optimum cavity length.

Figure 8 shows the effect of the particle radius on the response of the primary system. When the cavity length is small, the influence of the particle radius on the response is significant. The optimum value for the cavity length increases with increasing the particle radius. Figures 9(a) and 9(b) show the effects of the cavity height and the cavity width, respectively, on the response of the primary system. In both cases, it is clear that there is little influence of the cavity height or the cavity width on the response of the primary system.

### 6. CONCLUSIONS

The dynamics of an impact damper with granular materials in a horizontally vibrating system was investigated both experimentally and analytically. By means of the discrete element method, an analytical solution is provided to estimate, with reasonable accuracy,



the response of the primary system under sinusoidal excitation. In addition, the behavior of granular materials obtained by this method appears realistic. It is found that the damping efficiency depends on the particle material. It is also found that as the mass ratio increases, the response of the primary system decreases. Also, higher values of the mass ratio and particle radius result in the increase of the optimum cavity length.

#### REFERENCES

1. S. F. MASRI and T. K. CAUGHEY 1966 *American Society of Mechanical Engineers Journal of Applied Mechanics* **33**, 586–592. On the stability of the impact damper.
2. T. SATO, K. TANAKA, S. AIDA and Y. MOURI 1995 *JSME International Journal, Series C* **38**, 434–440. Vibration isolation in a system using granular medium.
3. Y. ARAKI, I. YOKOMICHI and J. INOUE 1985 *JSME* **28**, 1466–1472. Impact dampers with granular materials.
4. A. PAPALOU and S. F. MASRI 1996 *Earthquake Engineering and Structural Dynamics* **25**, 253–267. Response of impact dampers with granular materials under random excitation.
5. I. YOKOMICHI, Y. ARAKI, Y. JINNOUCHI and J. INOUE 1996 *American Society of Mechanical Engineers Journal of Pressure Vessel Technology* **118**, 95–103. Impact damper with granular materials for multibody system.
6. R. D. FRIEND and V. K. KINRA 2000 *Journal of Sound and Vibration* **233**, 93–118. Particle impact damping.
7. P. A. CUNDALL and O. D. STRUCK 1979 *Geotechnique* **29**, 47–65. A discrete numerical model for granular assemblies.
8. Y. TSUJI, T. TANAKA and T. ISHIDA 1992 *Powder Technology* **71**, 239–250. Lagrangian numerical simulation of plug flow of cohesionless particles in a horizontal pipe.